Stochastic dynamics of a non-linear cable–beam system

Jorge S. Ballaben, Rubens Sampaio & Marta B. Rosales

Journal of the Brazilian Society of Mechanical Sciences and Engineering

ISSN 1678-5878
Volume 38
Number 1

J Braz. Soc. Mech. Sci. Eng. (2016)
38:307-316
DOI 10.1007/s40430-015-0387-4

Springer

J Braz. Soc. Mech. Sci. Eng. (2016) 38:307–316
DOI 10.1007/s40430-015-0387-4

TECHNICAL PAPER

Stochastic dynamics of a non-linear cable–beam system

Jorge S. Ballaben[1,2] · Rubens Sampaio[3] · Marta B. Rosales[1,2]

Received: 15 December 2014 / Accepted: 20 June 2015 / Published online: 9 July 2015

Abstract Cable-stayed bridges and guyed towers are examples of structures extensively used in Civil Engineering. The uniform tension in the cable may change during service life due to various causes. Thus, uncertainty studies appear desirable to provide information about the effect of the parameter variations on the structure dynamics. The non-linear dynamic behavior of a cable-beam system, as a simplified model of a guyed structure, is studied. The beam behavior is assumed linear, while the cable is modeled with non-linear equations accounting for the extensibility and an initial deformed state. The deterministic equations are linearized about the reference configuration and then frequencies and modes are calculated. The modes are later used to construct a reduced order model. The non-linear equations are discretized by finite elements with a Galerkin procedure. Afterwards, a stochastic model is stated with the cable tension and beam stiffness assumed as random variables and appropriate probability density functions (PDFs) are derived through the Principle of Maximum Entropy. A numerical analysis is carried out using Monte Carlo techniques for simulations. Some unexpected features, such as multimodality of the PDFs, are observed. The structural model seems to be more sensitive to the cable tension uncertainty than to the beam stiffness.

Keywords Cable–beam structure · Non-linear models · Uncertainty quantification · PDF multimodality

1 Introduction

Guyed towers are frequently employed in Structural Engineering. The structure is set with a designed uniform tension in the cable that may be modified during the service life for different causes. The consequences of the change of parameters are diverse. For instance, a telecommunication guyed tower with guy tensions below the prescribed value can experiment operational difficulties due to the communication requirements. In effect, some signal transmission systems (e.g., point to point) are efficient within certain azimuth or zenithal motion tolerances. Then, any significant change in the motion of the tower at positions where the antennas and ancillaries are set causes the interruption in the signal transmission or a deterioration on the quality. Also, the structural behavior can be affected and failure may occur by fatigue. The beam stiffness can be a variable value as well. For example, in the case of guyed towers, various companies can share the use of the same supporting structure to install their antennas. In most of the cases, this situation requires the retrofit of the mast and one of the strategies consists in the partial reinforcement of the lattice mast legs. However, due to the construction procedures, the effective stiffness of the reinforced mast is not easy to

Technical Editor: Marcelo A. Trindade.

✉ Marta B. Rosales
mrosales@criba.edu.ar

Jorge S. Ballaben
jorgeballaben@gmail.com

Rubens Sampaio
rsampaio@puc-rio.br

[1] Department of Engineering, Universidad Nacional del Sur, Av. Alem 1253, 8000 Bahía Blanca, Argentina

[2] CONICET, Bahía Blanca, Argentina

[3] Department of Mechanical Engineering, PUC-Rio, Rua Marquês de São Vicente, 225, Rio de Janeiro, RJ 22451-900, Brazil

evaluate. Thus, a stochastic treatment of the mast stiffness seems appropriate. The guyed structure is modeled by a simplified cable–beam structure. Various authors have reported non-linear mathematical models of this system. Gatulli et al. [1, 2] have reported studies with the statement of a model that was used to solve non-linear dynamics and bifurcation problems. They state the differential equations and reduce them by a static condensation of the axial degree of freedom (DOF) of the cable. The cable is assumed to have non-linear behavior and the beam linear. Wei et al. [3] use the same model to perform a bifurcation analysis. Lenci and Ruzziconi [4] report other approach to solve the dynamics of a cable–beam structure that models the dynamics of a footbridge. These authors consider the non-linearities in both the beam and the cable.

In the present study, Gatulli's formulation is followed although with major changes, especially in the treatment of the equations. The beam model includes the axial deformation and no static condensation is performed in the cable equation. The system of partial differential equations is discretized by a finite element approach, which are first linearized to perform a natural frequency analysis. The frequencies and mode shapes correspond to global modes, though in some of them either the cable or the beam has a more relevant participation. Some of these modes are chosen as a basis for a Galerkin's projection. Thus, a non-linear, reduced order model is obtained which results very efficient to perform a stochastic study. For the sake of simplicity, two mode shapes are used in the reduction yielding a two-DOF model. Two stochastic models are constructed, one assuming the cable tension as a random variable (RV) and the other one with the bending stiffness as a stochastic parameter, respectively. In the first model, five different mean values of the tension are taken with the mean chosen within the range suggested by the standards ANSI/TIA-222-G [5] and CIRSOC 306 [6]. On the other hand, only one set of the bending stiffness RV (i.e., one mean value of the bending stiffness) is assumed in the second stochastic model. In order to select the probability density functions (PDF), the Principle of Maximum Entropy (PME) (Shannon [7]) is applied in each case. The PME states that, subjected to known constrains, the PDF which best represents the current state of knowledge is the one with largest entropy. Uncertainty propagation simulations are done with the two stochastic models. In the two cases, a gamma PDF is derived for both the cable tension and the bending stiffness. After an appropriate number of Monte Carlo simulations, the data is processed with statistical tools. Some plots of deterministic and stochastic responses are presented. An unexpected result is found when analyzing the PDF of the maximum displacements. In effect, multimodality is present for some of the tension cases. A similar result was obtained by the authors and co-workers in rather different problems [8, 9].

2 Analytical model of the non-linear cable-stayed beam

In order to analyze the dynamic characteristics and the uncertainty propagation on a cable-beam coupled system, a model consisting of a beam and a cable (Fig. 1) is studied. The cable is modeled neglecting the bending, torsional, and shear stiffnesses. In addition, the beam and cable are considered homogeneous and the system is constrained to oscillate in a plane.

Under the assumption of a small sag D to length L_c ratio (i.e., $D/L_c < 0.1$), the static equilibrium configuration can be approximated by a parabolic function in the cable

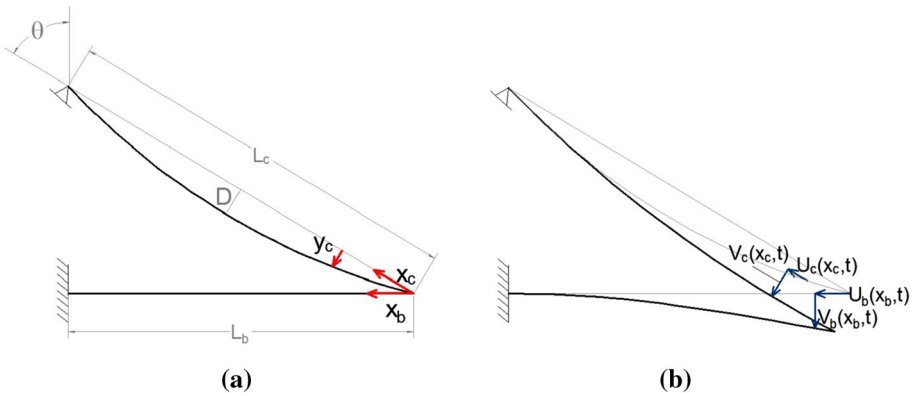

Fig. 1 Cable-stayed beam geometry and local coordinates. **a** static configuration; **b** dynamic configuration

domain, while the beam static deflection is assumed to be negligible. With respect to this reference configuration, and assuming an Euler–Bernoulli model of the beam, the actual plane configuration of the system at an instant t is completely described by the cable and beam displacement components $U_c(X_c,t)$, $V_c(X_c,t)$ and $V_b(X_b,t)$, $U_b(X_b,t)$, respectively, depicted in Fig. 1b.

The classical extended Hamilton's principle [10] is used to derive the non-linear equations of motion which govern the model dynamics and result in the following system

$$V_b : m_b\ddot{V}_b + c_b\dot{V}_b + EIV_b'''' = F_{v_b}(t,x_b)$$

$$U_b : m_b\ddot{U}_b + c_b\dot{U}_b + EA_bU_b'' = F_{u_b}(t,x_b)$$

$$V_c : m_c\ddot{V}_c + c_c\dot{V}_c - \left[HV_c' + EA_c\left(Y_c' + V_c'\right)\epsilon_c\right]' = F_{v_c}(t,x_c) \quad (1)$$

$$U_c : m_c\ddot{U}_c + \left[EA_c\epsilon_c\right]' = F_{u_c}(t,x_c)$$

with the following set of geometric and mechanical boundary conditions:

$$U_c(L_c) = V_c(L_c) = 0$$

$$V_b(L_b) = V_b'(L_b) = U_b(L_b) = 0$$

$$EIV_b''(0) = 0 \quad (2)$$

$$V_b(0) = -U_c(0)\cos\theta + V_c(0)\sin\theta$$

$$U_b(0) = U_c(0)\sin\theta + V_c(0)\cos\theta$$

$$EIV_b'''(0) + \left(EA_c\epsilon + H\right)\cos\theta + \left[EA_c\epsilon\left(y_c'(0) + V_c'(0)\right) + HV_c'(0)\right]\sin\theta = 0$$

The spacial and time derivatives are, respectively, denoted as $(*)' = d(*)/dx_c$ and $(\dot{*}) = d(*)/dt$, the beam and cable mass per unit length are m_b and m_c, respectively, $EI = E_bI_b$ is the beam flexural stiffness, $EA_c = E_cA_c$ and $EA_b = E_bA_b$ are the cable and beam axial stiffness, respectively, H is the mean static tension in the cable, Y_c is the initial configuration of the cable and, due the hypothesis of small sag to span ratio, $Y_c(x_c) = 4D\left(x_c/L_c - (x_c/L_c)^2\right)$, $\epsilon_c = U_c + Y_c'V_c' + 1/2V_c'^2$ is the expression of the cable elongation, $F_{v_b}(t,x_b)$, $F_{u_b}(t,x_b)$, $F_{v_c}(t,x_c)$ and $F_{u_c}(t,x_c)$ are the external force components (along the directions corresponding to the DOFs indicated by the subscripts), and θ is defined in Fig.1a. Usually in cable-stayed structures, the beam and the cable materials are assumed to have different viscous behavior. The model accounts separately for the beam and cable transverse damping per unit length, c_b and c_c, respectively; here an estimate of the system damping is assumed with the conventional values $c_i = 0.01(2m_i\omega_1)$, with $i = c,b$, and ω_1, the first natural frequency of the system.

Table 1 Values of the constants for Eqs. (1, 2) (beam)

L_b (m)	E_b (N/m^2)	$I_{b_{\text{mean}}}$ (m^4)	A_b (m^2)	m_b (kg)
10	2.1×10^{11}	3×10^{-6}	5×10^{-5}	39.25

Table 2 Values of the constants for Eqs. (1, 2) (cable)

L_c (m)	E_c (N/m^2)	A_c (m^2)	m_c (kg)	H_{mean} (N)	θ (degree)
10.77	1.56×10^{11}	3.44×10^{-5}	0.27	2800–5780	53.39

The values of the constants for the problem are given in Tables 1 and 2. The values of I_b and H are denoted with the "mean" subindex since they will be the reference parameters in the uncertainty study. Five values of the mean cable tension will be studied within the range reported in Table 2.

3 Reduced order model (ROM)

A reduced order model (ROM) is desirable to have an efficient tool that permits the uncertainty quantification. This reduction is done balancing two goals, a small dimension of the model and the main dynamic features retained. To achieve such a model, a Galerkin projection is formulated with the modal information obtained from a finite element discretization of the above-stated differential system.

3.1 Variational formulation

To introduce the variational formulation of the differential system of Eq. 1, let us define $\mathcal{V}$ as the set of (time dependent) basis functions and Φ as the set of weight functions. These sets must be selected from the space of functions with square integrable spatial derivatives which satisfy the essential boundary conditions defined in Eq. 2. The weak formulation consists in the projection of the space of functions $\mathcal{V}$, which are solutions of the Eq. 1, into the space of functions Φ, satisfying the following equation (i.e., the weak form):

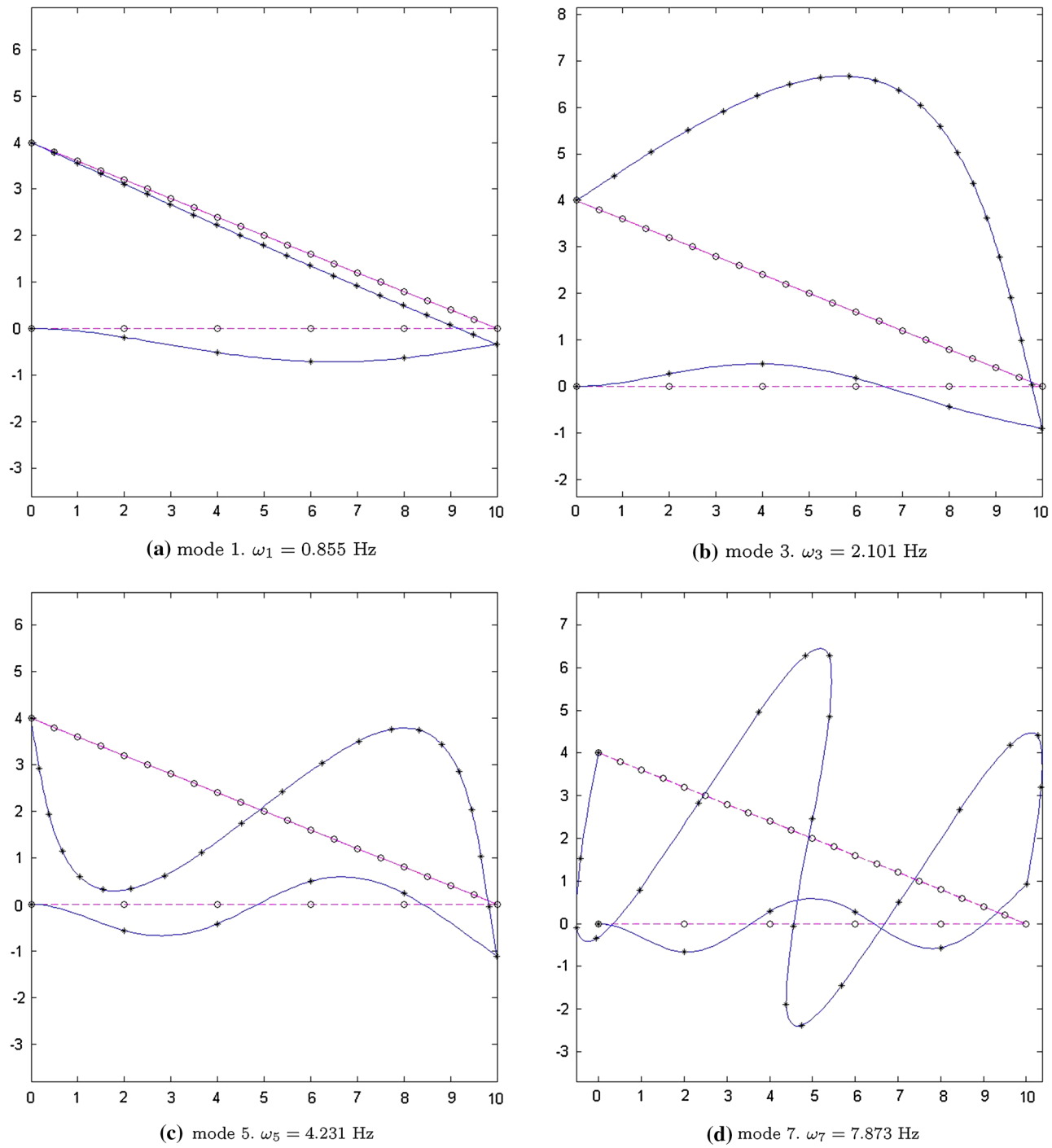

(a) mode 1. $\omega_1 = 0.855$ Hz

(b) mode 3. $\omega_3 = 2.101$ Hz

(c) mode 5. $\omega_5 = 4.231$ Hz

(d) mode 7. $\omega_7 = 7.873$ Hz

Fig. 2 Global modes and frequencies of the linearized cable-stayed beam

$$\mathcal{M}(\ddot{V},\phi) + \mathcal{C}(\dot{V},\phi) + \mathcal{K}_L(V,\phi) + \mathcal{K}_{NL}(V,\phi) = \mathcal{F}(V,\phi) + \mathcal{BC}, \tag{3}$$

where $\mathcal{M}$, $\mathcal{C}$, $\mathcal{F}$ are the mass, damping, and external force operators, respectively, while $\mathcal{K}_L$ and $\mathcal{K}_{NL}$ are the linear and non-linear stiffness operators and $\mathcal{BC}$ are the boundary operators. The variational forms of these quantities are written next:

$$
\begin{aligned}
\mathcal{M}(\ddot{V},\phi) &= \int_0^{l_b} m_b\left(\ddot{V}_b\phi_b + \ddot{U}_b\phi_b\right)\mathrm{d}x_b \\
&\quad + \int_0^{l_c} m_c\left(\ddot{V}_c\phi_c + \ddot{U}_c\phi_c\right)\mathrm{d}x_c \\
\mathcal{C}(\dot{V},\phi) &= \int_0^{l_b} c_b\left(\dot{V}_b\phi_b\right. \\
&\quad \left. + \dot{U}_b\phi_b\right)\mathrm{d}x_b + \int_0^{l_c} c_c\left(\dot{V}_c\phi_c + \dot{U}_c\phi_c\right)\mathrm{d}x_c \\
\mathcal{F}(V,\phi) &= \int_0^{l_b} \left(F_{U_b}\phi_b + F_{V_b}\phi_b\right)\mathrm{d}x_b \\
&\quad + \int_0^{l_c} \left(F_{V_c}\phi_c + F_{U_c}\phi_c\right)\mathrm{d}x_c \\
\mathcal{K}_L(V,\phi) &= \int_0^{l_b} \left(EI_bV_b''\phi_b'' - P_HV_b'\phi_b' + EA_bU_b'\phi_b'\right)\mathrm{d}x_b \\
&\quad + \int_0^{l_c} \left(HV_c'\phi_c' + EA_cU_c'\phi_c'\right)\mathrm{d}x_c \\
\mathcal{K}_{NL}(V,\phi) &= \int_0^{l_c} EA_c\left[\left(Y_c' + V_c'\right)\left(U_c' + Y'V_c' + \frac{V_c'^2}{2}\right)\phi_c'\right. \\
&\quad \left. + \left(Y_c'V_c' + \frac{V_c'^2}{2}\right)\phi_c'\right]\mathrm{d}x_c \\
\mathcal{BC} &= \left[HV_c' + EA_c\left(Y_c' + V_c'\right)\left(U_c' + Y_c'V_c' + V_c'^2/2\right)\right]\phi_c\big|_0^{l_c} \\
&\quad + EA_c\left(U_c' + Y_c'V_c' + V_c'^2/2\right)\phi_c\big|_0^{l_c} + EI_bV_b'''\phi_b\big|_0^{l_b} \\
&\quad - EI_bV_b''\phi_b'\big|_0^{l_b} + P_HV_b'\phi_b\big|_0^{l_b} + EA_bU_b'\phi_b\big|_0^{l_b}
\end{aligned}
\tag{4}
$$

P_H is the horizontal component of the cable pretension force, and it is involved in the beam second order effect (decrease of beam stiffness due to axial load).

After a convenient linearization, the normal mode shapes of the system were taken as the base for the construction of the ROM. Due the difficulty to solve analytically the eigenvalue problem of the system (1, 2), an ad hoc linear finite element discretization was carried out. The beam was discretized with five standard 6-DOF beam elements and the cable with ten 6-DOF (3-node) prestressed cable elements. Figure 2 depicts the first normal—global—modes of the structure.

3.2 Reduced order model formulation

The non-linear continuous cable–beam system governed by Eqs. (1–2) is reduced to a 2-DOF system through a Galerkin discretization. Both local and global modes, found from the previous FEM eigenvalue analysis, can be distinguished. In the first ones, only one of the substructures is involved (either the cable or the beam). On the contrary, the global modes are related with the whole structure (both the cable and the beam). Here, the first two global modes (modes 1 and 3, Fig. 2) are selected in order to introduce more information in the ROM. The displacements have been expressed in terms of the modal space basis as $v = \boldsymbol{\Phi} q$, where the displacement vector $v = \{V_b(x_b,t), U_b(x_b,t), V_c(x_c,t), U_c(x_c,t)\}^T$, the modal matrix $\boldsymbol{\Phi} = [\boldsymbol{\phi}_1 | \boldsymbol{\phi}_2]$ whose components are the eigenfunctions $\boldsymbol{\phi}_i = \{\phi_{b_v i}(x_b), \phi_{b_u i}(x_b), \phi_{v_c i}(x_c), \phi_{u_c i}(x_c)\}^T$, and the modal amplitude vector $\boldsymbol{q} = \{q_1(t), q_2(t)\}^T$. After imposing the stationarity of the associated Hamiltonian, the following non-linear ordinary differential equations are obtained:

$$
\begin{cases}
m_1\ddot{q}_1 + a_1\dot{q}_1 + c_1q_1 + c_2q_2 + c_{12}q_1q_2 + c_{11}q_1^2 \\
+c_{22}q_2^2 + c_{211}q_1^2q_2 + c_{122}q_1q_2^2 + c_{111}q_1^3 + c_{222}q_2^3 \\
= p_1\cos(\omega t) m_2\ddot{q}_2 + a_2\dot{q}_2 + d_1q_1 + d_2q_2 \\
+d_{12}q_1q_2 + d_{11}q_1^2 + d_{22}q_2^2 + d_{211}q_1^2q_2 + d_{122}q_1q_2^2 \\
+d_{111}q_1^3 + d_{222}q_2^3 = p_2\cos(\omega t)
\end{cases}
\tag{5}
$$

The coefficients of the above equations are included in the Appendix.

A ROM is a useful tool to reduce drastically the computing time. This feature is potentially attractive to perform an uncertainty quantification analysis. For instance, it took 30 min of CPU to simulate the non-linear system obtained from the finite element discretization by the Galerkin procedure, while the simulation of the ROM took 4 min, using the same computer.

4 Uncertainty quantifications

Uncertainty quantifications with two stochastic parameters are now performed with the above-stated non-linear ROM. The initial tension of the cable (H) and the second area moment of the cross section (I_b, proportional to the beam stiffness EI_b) are the random parameters under consideration. Monte Carlo simulations are carried out taking H and I_b as RV separately. Five cases of mean initial pretension (H_{mean}) are taken into account while a single value of mean beam stiffness ($I_{b\text{mean}}$) is considered. For each study, the PDF is chosen by means of the PME. Further interpretations of this principle can be found in [11, 12]. The PME states that, subjected to known constraints, the PDF which best represents the current state of knowledge is the one with largest entropy S. The measure of uncertainty of a RV X is defined by the following expression:

$$
S\left(f_X\right) = -\int_D f_X(X) log\left(f_X(X)\right)\mathrm{d}X, \tag{6}
$$

in which f_X stands for the PDF of X and D is its domain. It is possible to demonstrate that the application of the PME under the constraints of positiveness and bounded second moment, leads to a gamma PDF. Both the cable tension and the bending stiffness fulfill these conditions.

A gamma distribution with parameters a and $b\left(\mu_X = ab\,; \sigma_X^2 = ab^2\right)$ is given by the next expression:

$$
f(x) = \frac{1}{b^a\Gamma(a)}x^{a-1}e^{\frac{-x}{b}}. \tag{7}
$$

Consequently, the variables H and I_b are distributed according to a gamma distribution. The parameters of the distribution are found after the mean and standard deviation of the RVs are specified. Applications of the PME in structures can be seen in [13–16].

4.1 Initial pretension force on the cable

The pretension force of the cable is, sometimes, not easy to measure. Also, in real structures changes in the pretension values due to weather, temperature, and other actions, cause variations in this parameter throughout the service life. Thus, the propagation of this uncertainty in the structural behavior can be performed with a stochastic study. Here, five sets of the RV H (each with a different H_{mean}) are analyzed. The lowest value of H_{mean} corresponds to the suggested value of the Argentinian code CIRSOC 306 [6], which results in $H_{\text{mean}} = 2800$ N. The other four values were calculated from the ANSI/TIA [5] code that proposes to use values ranging from the 8 to the 15 % of the cable ultimate strength (σ_R), yielding $0.08\sigma_R Ac = 3300$ N, $0.1\sigma_R Ac = 4130$ N, $0.12\sigma_R Ac = 4950$ N, and $0.14\sigma_R Ac = 5780$ N. The adopted standard deviation, for all the cases, is $\sigma_{\text{H}} = \text{H}_{\text{mean}}/5$.

4.2 Beam stiffness

The beam stiffness appears to be a fixed parameter that does not change along the service life of the structure. Then, no uncertainty quantification study would be necessary. However, events, such as eventual differences between the design value and the real beam stiffness together with the possibility of reinforcement of the beam or degradation on the stiffness due to different mechanisms, make an uncertainty propagation study appropriate. Here, a single case of I_{mean} is considered, but its influence is studied for all the cases of H_{mean}. The standard deviation used for the gamma distribution is $\sigma_{I_b} = I_{b\text{mean}}/5$. In what follows, we will refer to the bending stiffness EI_b also as a random quantity though actually the RV is I_b.

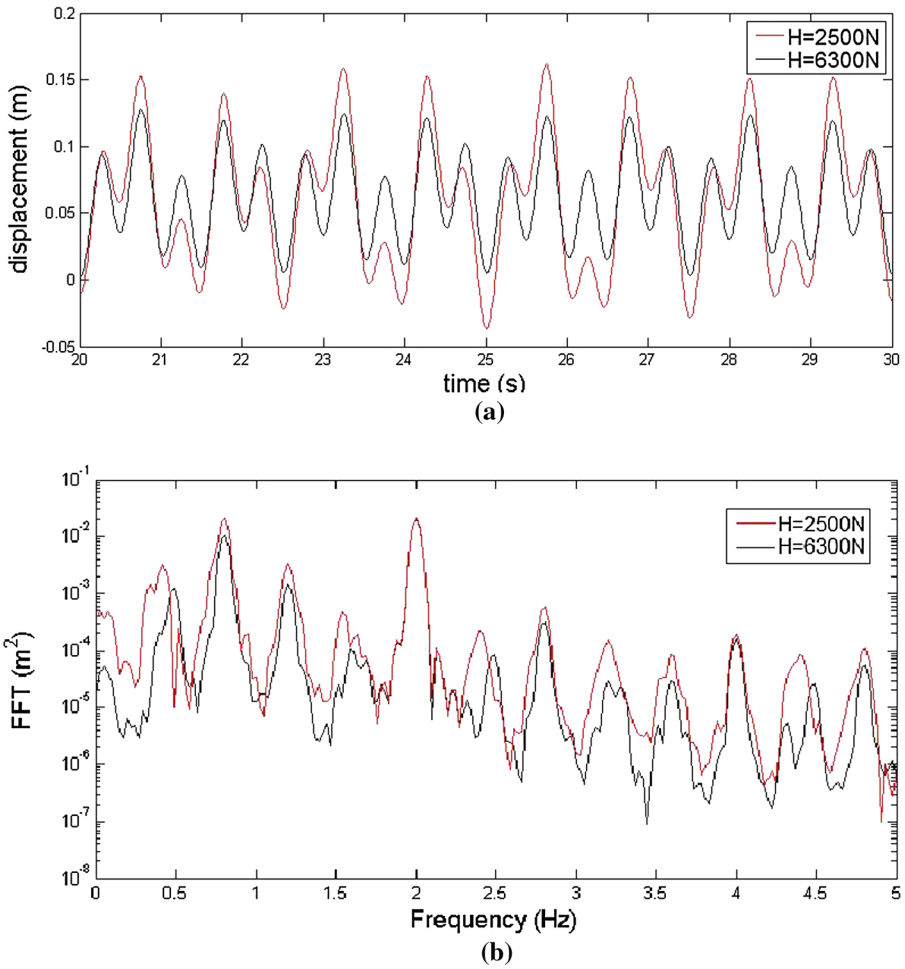

Fig. 3 Transverse displacement of the beam at point $x_b = 4$ m found with the deterministic ROM for the extreme cases of H. **a** Trajectory of displacements; **b** FFT

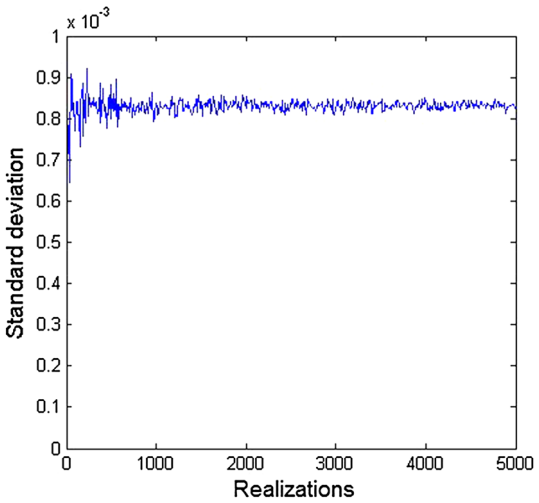

Fig. 4 Convergence of the standard deviation of the transverse displacement in Monte Carlo simulations

4.3 Load

In this study, a transverse load uniformly distributed on the beam is considered in addition to the self-weight of the structural components. A cosine function is employed to simulate dynamic load. The load magnitude $\bar{F}_{v_b} = 1700$ N is chosen to obtain compatible maximum displacements with the linear beam theory used in the problem statement and the frequency of the excitation, $\omega = 2$ Hz, to avoid resonance effects.

5 Results

In this work, for the sake of brevity, only results of the beam transversal displacements are presented. All the results correspond to the coordinate $x_b = 4$ m (see Fig. 1), the point where maximum transversal displacements occur. The length of the simulation is 30 s for each run. Figure 3a depicts a 10 s sample of the transverse displacement for the extreme cases of initial pretensions. Figure 3b shows the result of a FFT analysis of the same cases. Both results illustrated in Fig. 3 (and all the intermediate ones) exhibit a similar shape, with two main peaks, one corresponding to the load frequency and other one close to 0.80 Hz.

To achieve significant statistical results, a convergence study on the standard deviation of the displacement was performed to determine the minimum number of realizations of the Monte Carlo simulations. Figure 4 shows a typical result of the convergence study. It can be observed

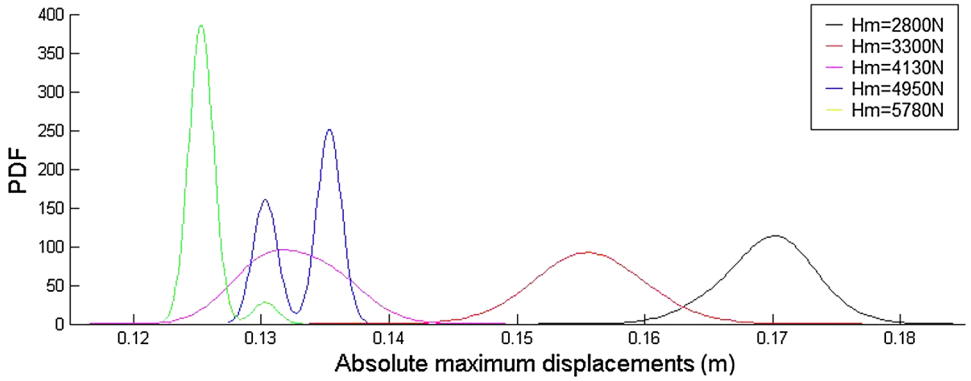

Fig. 5 PDF of absolute maximum displacements of the beam at $x_b = 4$ m with stochastic variable H, for each H_{mean}

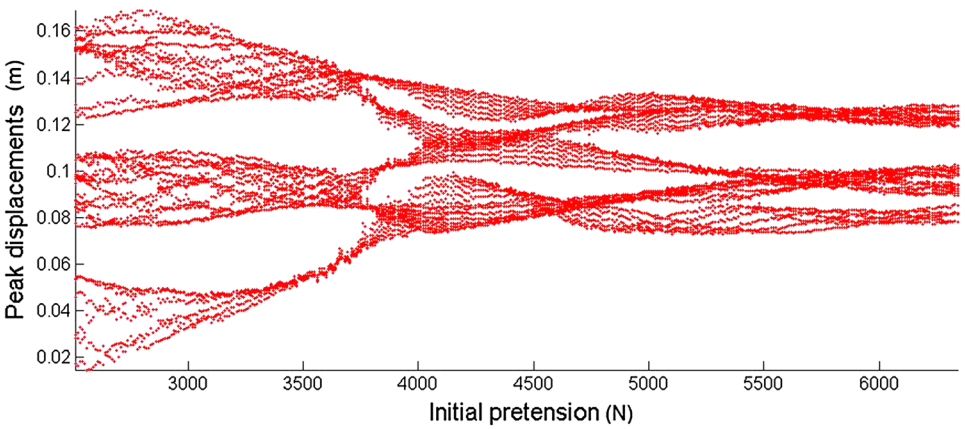

Fig. 6 Deterministic model. Peak values of displacement at $x_b = 4$ m versus initial pretension

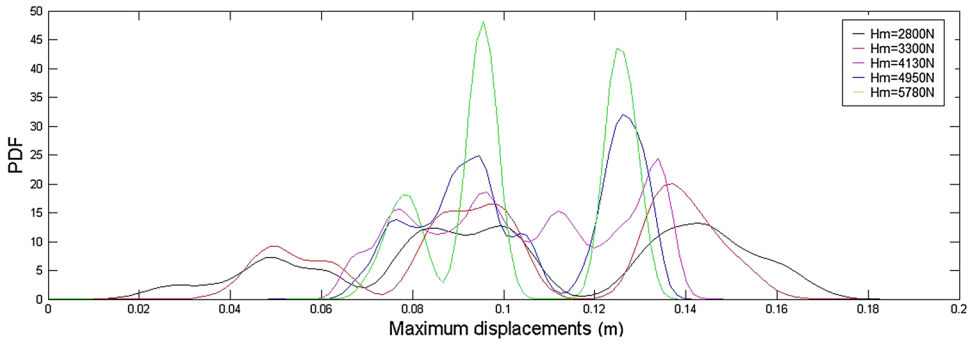

Fig. 7 Stochastic model. PDF of peak values of displacements at $x_b = 4$ m

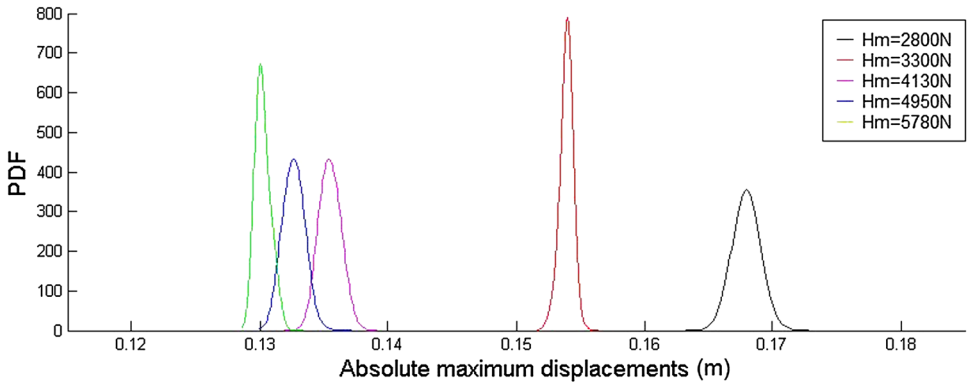

Fig. 8 PDF of absolute maximum values of displacements at $x_b = 4$ m, with I_b as a stochastic variable, for each H_{mean}

that at least 2500–3000 realizations are required to achieve convergence of the standard deviation.

5.1 Initial pretension as a stochastic variable

The absolute maximum values of the transverse displacement at $x_b = 4$ m are statistically studied. Figure 5 shows the PDF of these maximum displacements for each case. The curves were numerically generated using the *ksdensity* function of MATLAB. This tool allows to approximate a PDF shape from the histograms through an algorithm the so-called *kernel smoothing function estimate*. For the three smaller values of H_{mean}, similar shapes with approximately the same deviation on the results are obtained. A particularity is observed: there is a rather large separation between the modes of the case of $H_{\text{mean}} = 3300$ N (in red) and 4130 N (in magenta). Multimodality is apparent on the cases of 4950 N (in blue) and 5780 N (in green). There is a important change in the variation between the three cases with the smaller H_{mean} and the other two. Other remarkable point is that the difference between the cases of 4130 and 4950 N is not only a shift of the PDF along the displacement axis (as the other cases) but also a change in the same region, consisting in a drastic reduction of the dispersion and a variation to multimodality; this feature represents a clear qualitative change on the statistics of the absolute maximum values of the transversal displacement which can be regarded as a stochastic bifurcation.

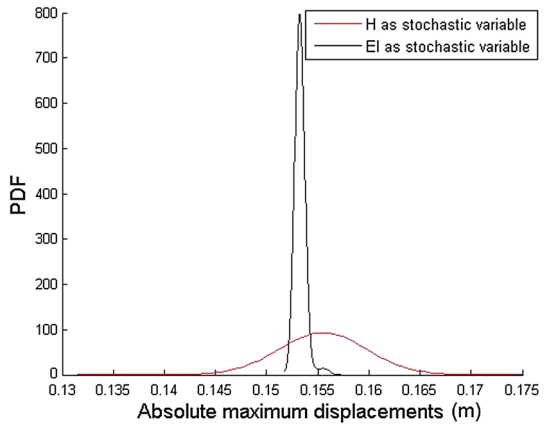

Fig. 9 PDF of absolute maximum values of displacements at $x_b = 4$ m, for $H_m = 3300$ N, varying H (*red*) and EI_b (*black*) (color figure online)

Figure 6 shows a deterministic plot and depicts the local peak values for each realization in the range of studied initial pretensions. It shows that although only two relevant peaks are observed (see Fig. 3b), a rather complex plot is obtained. One can notice a change from three well-defined branches in the range 2500–4000 N to a single branch within 4000–4500 N and what seems to be a transition zone to three branches after 4500 N. The different types of PDF (and the behavior of the PDF when changing the H_{mean}) observed in Fig. 5 agree with the ranges of H_{mean} with distinctive patterns (three branches, one branch, or a

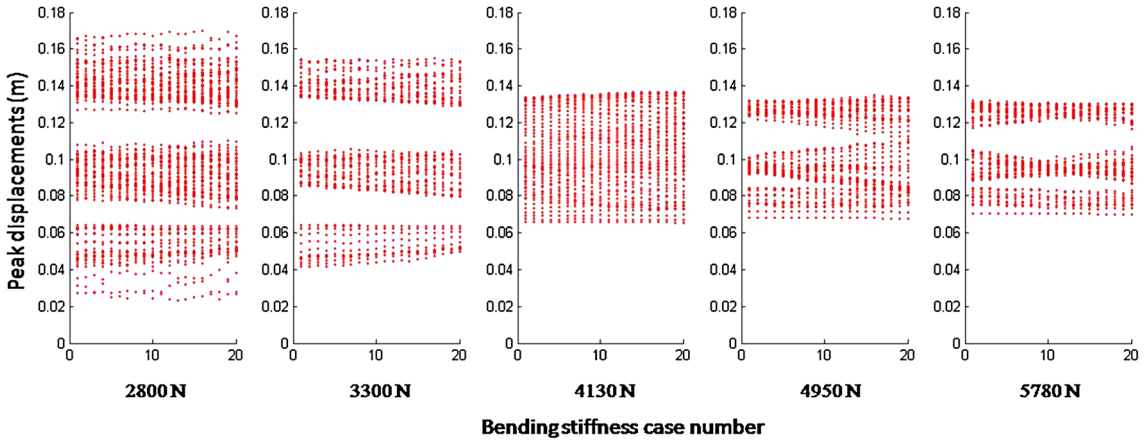

Fig. 10 Deterministic model. Peak values of displacement at $x_b = 4$ m versus EI_b

transition region). The dynamics of the non-linear deterministic problem affects directly the stochastic results. It must be recalled that Fig. 6 includes the plots of all the peaks on each realization, and the Fig. 5 contains the statistics of the absolute maximum peak of each realization.

To end with the analysis of the results with the initial pretension as a RV, Fig. 7 shows the PDF for the peaks (local maximums) of the realizations. As expected, the resulting PDFs have larger variability than the one observed in Fig. 5; all the results are multimodal and the modes approximately correlate with the branch or branches at the corresponding H_{mean} region of Fig. 6. That is, the range of the H_{mean} should be compared in the two figures; in Fig. 7, the range is given by colors and in Fig. 6 by the horizontal scale.

5.2 Beam stiffness as a stochastic variable

Here, the bending stiffness is assumed stochastic and the H is fixed. Five cases were analyzed, assuming $H = H_{\text{mean}}$ for the five tension cases proposed in the previous study. Figure 8 shows the PDF for the maximum displacements, at $x_b = 4$ m, for each case of H. A "gap" between the modes of the $H = 4130$ N and $H = 4950$ N cases is present. The standard deviation is drastically less than the previous study in which H was considered stochastic. This indicates that the system has a robust behavior (regarding the absolute maxima) to changes of the beam stiffness. In other words, the expected maximum value almost does not change when the value of beam stiffness is statistically varied. The difference on the variation found for the study varying EI_b and varying H is depicted in Fig. 9. It can be observed that the PDF modes do not match. Similar conclusions are found for the other cases not shown here.

Figure 10 shows a deterministic plot and depicts the local peak values for each realization in the range of studied beam stiffness for each case of H. It is clear that the absolute maxima almost do not change when the value of EI_b is varied, at least within the range under study. The general behavior and size of the peaks branches remain the same than those of Fig. 6 for the a, b, and c cases of Fig. 10 and show some differences on d and e sets. An interesting result is that the PDF of the peaks, when EI_b is considered stochastic is totally similar to the ones found when H is assumed stochastic.

6 Conclusions

In this work, a non-linear formulation of a cable-stayed beam structure was presented. First, a deterministic model was stated and the governing system discretized via a finite elements method. A 2-DOF ROM of the system was then constructed using eigenvalue results obtained from a linearization. Once calibrated, an uncertainty propagation using (separately) the initial pretension of the cable and the beam stiffness as stochastic parameters was performed with the ROM. The PDFs of the statistic parameters were chosen using the PME and a gamma PDF was obtained for both cases. Monte Carlo simulations were employed to solve the system.

The stochastic tension study considered five cases with different values of H_{mean} were analyzed. The PDFs of absolute maximum displacements of the beam were studied and noticeable differences were found in the deviation, shapes, and modes. Two remarkable cases occur between the cases $H_{\text{mean}} = 3300$ and 4130 N a rather large "gap" is observed. On the other hand, there is no shift of the PDFs when $H_{\text{mean}} = 4130$ and 4950 N though they exhibit less dispersion and a change to bimodality is apparent.

A deterministic study of the variation of the peaks with the initial pretension was also carried out, and at least, three

regions with different behaviors are recognized. Also, the most remarkable changes in the PDF of the maximum values occur when the H_{mean} value changes from one zone to other. The PDFs of the peaks values were also studied.

When the beam stiffness was chosen as the stochastic parameter, the PDF of the absolute maximum displacement values shows a notable reduction on the dispersion with respect to the results obtained when H was assumed stochastic. The beam stiffness seems to have less influence on the absolute maximum displacements in this system. The PDFs of peak values are analogous to the ones obtained in the stochastic tension study.

Acknowledgments The authors acknowledge the financial support from CONICET, MINCyT, and UNS (Argentina) and CAPES, CNPq, and FAPERJ (Brazil).

Appendix

The constants of Eq. 5 are listed next. For the sake of brevity, a compact notation is introduced. For instance, if one needs to calculate d_{211}, then, as stated in the fourth line, $L^2 = d$, and afterwards, in the sixth line, L^i_{jkk} with $i = 2$, $j = 2$ and $k = 1$ gives $L^2_{211} = d_{211}$.

$$
\begin{aligned}
m_i =& m_b \int_0^{L_b} \phi'^2_{b_v i} + \phi'^2_{b_u i} dx_b + m_c \int_0^{L_c} \phi'^2_{c_v i} + \phi'^2_{c_u i} \mathrm{d}x_c \\
a_i =& c_b \int_0^{L_b} \phi'^2_{b_v i} + \phi'^2_{b_u i} dx_b + c_c \int_0^{L_c} \phi'^2_{c_v i} + \phi'^2_{c_u i} \mathrm{d}x_c \\
p_i =& \int_0^{L_b} P_{b_v i}\phi_{b_v i} + P_{b_u i}\phi_{b_u i} dx_b + \int_0^{L_c} P_{c_v i}\phi_{c_v i} + P_{c_u i}\phi_{c_u i} \mathrm{d}x_c \\
L^1 =& c, L^2 = d \\
L^i_{kkk} =& \frac{1}{2} EA_c \int_0^{L_c} \phi'^3_{c_v k}\phi'_{c_v i} \mathrm{d}(x_c) \\
L^i_{jkk} =& \frac{3}{2} EA_c \int_0^{L_c} \phi'^2_{c_v k}\phi'^2_{c_v j}\phi'_{c_v i} \mathrm{d}(x_c) \\
L^i_i =& \int_0^{L_b} \left\{ EI\phi''^2_{b_v i} + EA_b\phi'^2_{b_u i} \right\} dx_b + \int_0^{L_c} \left\{ H\phi'^2_{c_v i} + EA_c\phi'^2_{c_u i} \right. \\
&+ \left. 2EA_c Y'_c \phi'_{c_u i}\phi'_{c_v i} + 2EA_c Y'^2_c \phi'^2_{c_v i} \right\} \mathrm{d}x_c \\
L^i_j =& \int_0^{L_c} EA_c \left(Y'_c \phi'_{c_u j}\phi'_{c_v i} + Y'^2_c \phi'_{c_v j}\phi'_{c_v i} + \phi'_{c_v j}\phi'_{c_u i} \right) \mathrm{d}x_c \\
L^i_{12} =& \int_0^{L_c} \left\{ EA_c \left(3Y'_c \phi'_{c_v 1}\phi'_{c_v 2}\phi'_{c_v i} + \phi'_{c_u 1}\phi'_{c_v 2}\phi'_{c_v i} + \phi'_{c_u 2}\phi'_{c_v 1}\phi'_{c_v i} \right. \right. \\
&+ \left. \left. Y'_c \phi'_{c_v 1}\phi'_{c_v 2}\phi'_{c_u i} \right) \right\} \mathrm{d}x_c \\
L^i_{jj} =& \int_0^{L_c} EA_c \left(\frac{3}{2} Y'_c \phi'^2_{c_v j}\phi'_{c_v i} + \phi'_{c_v j}\phi'_{c_u j}\phi'_{c_v i} + \frac{1}{2}\phi'^2_{c_v j}\phi'_{c_u i} \right) \mathrm{d}x_c \\
& \text{with} \quad i, j, k = 1, 2.
\end{aligned}
$$

References

1. Gattulli V, Lepidi M (2003) Nonlinear interactions in the planar dynamics of cable-stayed beam. Int J Solids Struct 40:4729–4748
2. Gattulli V, Lepidi M, Macdonald JHG, Taylor CA (2005) One-to-two global-local interaction in a cable-stayed beam observed through an analytical, finite element and experimental models. Int J Non-Linear Mech 40:571–588
3. Wei MH, Xiao YQ, Liu HT (2011) Bifurcation and chaos of a cable-beam coupled system under simultaneous internal and external resonances. Nonlinear Dyn 67:1969–1984
4. Lenci S, Ruzziconi L (2009) Nonlinear phenomena in the single mode dynamics of a cable supported beam. Int J Bifurc Chaos 19(3):923–945
5. ANSI/TIA-222-G (2009) Structural standard for antenna supporting structures and antennas. Telecommunications Industry Association, Arlington
6. CIRSOC 306 (1992) Estructuras de Acero Para Antenas. INTI, BuenosAires
7. Shannon C (1948) A mathematical theory of communication. Bell Tech J 27:379–423
8. Pagnacco E, Sampaio R, Souza de Cursi JE (2011) Frequency response functions of random linear mechanical systems and propagations of uncertainties. Mec Comput 30:3357–3380
9. Buezas FS, Rosales MB, Sampaio R (2013) Propagation of uncertainties and multimodality in the impact problem of two elastic bodies. Int J Mech Sci 75:145–155
10. Fung YC (1965) Foundations of solid mechanics. Prentice-Hall Inc, New Jersey
11. Udwadia FE (1989) Some results on maximum entropy distributions for parameters known to lie in finite intervals. SIAM Rev 31(1):103–109
12. Singh V (2013) Entropy theory and its application in environmental and water engineering. Wiley, Chichester
13. Kapur JN, Kesavan HK (1992) Entropy optimization principles with applications. Academic Press Inc, New York
14. Ritto TG, Sampaio R, Cataldo E (2008) Timoshenko beam with uncertainty on the boundary conditions. J Braz Soc Mech Sci Eng 30(4):295–303
15. Sampaio R, Cataldo E (2010) Comparing two strategies to model uncertainties in structural dynamics. Shock Vib 17(2):171–186
16. Dorini FA, Sampaio R (2012) Some results on the random wear coefficient of the Archard model. J Appl Mech 79:051008–051014